COMPARING THE PERFORMANCE OF COLLABORATIVE AND COMPETITIVE MARKET OF RIDE-SHARING SYSTEM: A DYNAMIC GRAPH-BASED METHOD

Xin Dong*, **Corresponding Author**
Department of Civil and Environmental Engineering
The Pennsylvania State University
231 Sackett Building
University Park, PA 16802
xjd5036@psu.edu
phone: 814-996-9601

Jose Ventura
Department of Industrial and Manufacturing Engineering
The Pennsylvania State University
356 Leonhard Building
University Park, PA 16802
jav1@psu.edu

Vikash V. Gayah
Department of Civil and Environmental Engineering
The Pennsylvania State University
231 Sackett Building
University Park, PA 16802
gayah@engr.psu.edu

Word Count: 6470 words + 3 table(s) × 250 = 7220 words

Submission Date: July 30, 2024

Abstract

Ride-sharing platforms like Uber and Lyft have transformed urban transportation by reducing travel distances and increasing vehicle occupancy rates. However, efficiency is often limited by market segmentation, where rider-rider pairs are restricted to specific platforms, potentially leading to suboptimal results. This study uses a dynamic graph-based framework with maximum weighted matching to compare the efficiency of a competitive market with a more collaborative one where platforms can share individual trip requests. We model riders as graph vertices with dynamic weighted edges representing profit and waiting times. The competitive market is modeled as sub-graphs representing different platforms, the collaboration scenario as a union graph, and a rational collaboration mode as a partial union graph under Shapley-value-based profit constraints and information transparency control. Maximum weighted matching is found within sub-graphs for the competitive market and within the union graph for different collaboration types. Additionally, we examine how the computational performance varies with the scale of nodes and edges. The results reveal that a collaborative market significantly improves share rates and profit while reducing travel distances and waiting times by overcoming market segmentation barriers. This highlights the benefits of cross-platform collaboration, suggesting it can enhance operational efficiency in a competitive environment. Although market segmentation and platform controls can impact performance, rational collaboration generally serves as a feasible approach to achieving a near-ideal fully collaborative scenario.

Keywords: On-demand Ride-sharing, Market Segmentation, Competition, Collaboration, Maximum Weighted Matching, Shapley Value

INTRODUCTION

Ride-sharing involves sharing a vehicle journey among riders traveling in similar directions, thereby reducing the number of vehicle trips needed to serve passengers (*1*). This concept can be traced back to the push for carpooling during the US oil crisis in the 1970s (*2*). Since then, it continuously evolved and been promoted in various forms, such as peer-to-peer ride-sharing (*3*) and on-demand ride-sharing (*4*). The push for ride-sharing stems from its numerous benefits, including reducing total vehicle travel distance, increasing vehicle occupancy rates, decreasing required fleet size, alleviating traffic congestion, and lowering greenhouse gas emissions (*5*). The sharing mobility economy has grown considerably in recent years and achieved over $130 billion in global consumer spending (*6*) in 2019 (pre-pandemic). Various Transportation Network Companies (TNCs) offer ride-sharing services and compete for customers, including Uber, Lyft, DiDi, and Via.

Competition among TNCs is not always beneficial, as a competitive market can lead to either competitive prices or price collusion for ride services (*7*). Competitive prices alter riders' selection of platforms, while price collusion (usually resulting in surged prices during peak hours) tends to push riders away to seek other options. This potential dynamic of riders' shifting among platforms brings instability to the segmentation of the system and impedes the economies of scale for each platform. The economies of scale originally refer to cost advantages that enterprises obtain due to the increase in the scale of operation (*8*). In ride-sharing systems, it refers to the efficiency increases as the amount of service increases. Specifically, as the number of shared ride requests increases, various measures of system performance (e.g., service quality, sharing rate, detour distance—the extra distance in a shared trip compared with the corresponding rider's single trip—, and wait time) improve (*9, 10*). The fragmented ride-sharing market created by various TNCs divides users into separate matching pools, reducing the potential for higher efficiency and quality (*11*) that can be achieved due to economies of scale.

Collaboration among on-demand service platforms might be a potential solution to mitigate these inefficiencies. In the practical experience of the ride-hailing services market, where matching typically involves pairing one rider with one driver, established practices already exist. For instance, the Uber platform has partnered with taxi-hailing companies such as Curb, Arro, Flywheel, and YoTaxi to integrate traditional taxi options into their applications (*12, 13*). This initiative aims to boost matching efficiency and service coverage by integrating their resources. Some third-party platform integrations also exist; for example, Baidu Map integrates the platform options of DiDi and others in a single interface for ride-hailing in China (*14*). This integration has resulted in a lower pickup distance and a higher match rate. However, there are no established practices for ride-sharing matching collaboration in practice. Some research on this domain does exist, details will be presented in the next section.

This paper introduces a dynamic graph-based framework to compare the performance of ride-share systems under different levels of collaboration among TNC platforms. The dynamic weighted graph captures the status of rider requests and tracks rider waiting times, which are used to make matching decisions. The Shapley value method allocates profits for inter-platform rider pairs and compares them with intra-platform profits. If inter-platform profit is higher, the collaboration option is agreed upon. To this end, rider-rider matching pairs selected based on the maximum weighted matching method within and across platforms are recorded and processed. Our goal is to maximize the total saved travel distances in shared trips and minimize the total wait time of riders. The performance of this framework is compared to both a perfect competition scenario and a complete collaboration scenario through empirical experiments.

The rest of this paper is organized as follows. The next section reviews the literature on both traditional and state-of-the-art technologies, highlighting existing gaps in ride-sharing systems. This is followed by a detailed methodology section. The following section presents an empirical experiment using the New York City Taxi and Limousine Commission (TLC) dataset, comparing the performance of competitive and collaborative markets. Finally, the last section concludes with our findings.

LITERATURE REVIEW

In this section, we review the literature focusing on two main streams. The first stream addresses matching in ride-sharing systems, emphasizing the matching among riders (shareability) rather than the matching between rider pairs or riders and drivers (dispatching process). The second stream focuses on collaboration within the ride-sharing market, examining two key areas: the effects of competition and collaboration, and the existing collaboration methods and their impacts on the market. Additionally, we clearly state our contributions to the field.

Matching in Ride-sharing System

There is a wide spectrum of approaches to solving matching problems in ride-sharing systems, including heuristic, combinatorial optimization, machine learning, and graph-based methods.

For carpooling and peer-to-peer ride-sharing services, where demand is well determined far in advance of trips, the aforementioned solutions are easy to implement (*15–17*). However, demand is generated shortly before trip departure in on-demand ride-sharing systems; matching decisions must be made dynamically. In this context, heuristic methods, sometimes referred to as instant matching methods, offer the advantage of near-instant responses (*18, 19*), but suboptimum solutions (e.g., higher total vehicle travel distances and lower successful pooling rates). To handle this, combinatorial optimization methods (such as integer linear programming and dynamic programming) combined with sliding windows (*20*) are widely used. These approaches involve optimizing the assignment of a batch of requests at regular time intervals and continuously updating decisions as new data comes in (*21, 22*). Although combinatorial optimization methods are capable of providing system optimum solutions (*23*), their application can still be computationally expensive and complex.

In comparison, numerous polynomial-time graph-based algorithms can be applied to matching problems. For a detailed review of these types of models, readers are referred to Duan (*24*). Bipartite matching is widely used for finding rider-driver pairs; e.g., Agatz et al. developed a dynamic ride-matching optimization method by positioning passengers and drivers on two sides of a bipartite graph (*25*). General graphs are more suitable for finding rider-rider pairs. Depending on the objectives, the matching problem can be categorized into maximum cardinality matching (containing as many edges as possible) or maximum weighted matching (MWM). Some papers have applied maximum cardinality matching to maximize the possibility of riders being matched in a ridesharing system, for example, Santi et al. (*26*). Instead of finding maximum cardinality matching, we focus on finding MWM in a general graph. Galil's $O(mn \log n)$-time algorithm for maximum weighted matching in general graphs (*27*) is efficient for sparse graphs. This efficiency makes graph-based methods valuable in systems with frequently changing configurations.

Most developed matching models in ride-sharing systems have focused on a single TNC, overlooking the potential for shareability among different platforms. Our paper, however, focuses on rider-matching both within and among platforms. Besides, unlike most papers that use bipar-

tite graph matching, maximum cardinality matching in unweighted general graphs, or MWM in weighted general graphs that only consider travel time, we propose a dynamic graph that maximizes total profit while prioritizing riders with longer waiting times.

Platform Competition and Collaboration

Several studies have examined the impact of competition among TNC platforms. For example, Séjourné et al. quantified how demand fragmentation degrades the efficiency of the Mobility-on-Demand services systems by focusing on the supply re-balancing costs incurred by this demand fragmentation (*28*). Liu et al. examined competition's impact on travel characteristics and introduced entropy to evaluate spatial and temporal competition among TNC platforms (*11*). The study found that increased competition leads to decreased share rates on each platform and longer average travel distances for shared trips.

Other studies have investigated how collaboration influences system efficiency and platform profit. Zhou et al. presented the equilibrium of a competitive ride-sourcing market with platform integration and compared the performance of the ride-sourcing market with and without integration (*29*). The study found that platform integration does not always increase platform profit but always enhances social welfare. Guo et al. proposed different profit allocation mechanisms among TNC platforms in four market structures, demonstrating benefits such as reducing total vehicle travel distance and decreasing the total number of trips in collaborative scenarios (*30*). The focus was primarily on profit allocation mechanisms for different market designs and emphasizing the required fleet size. Wang et al. introduced a deep reinforcement learning model to determine driver-passenger pairs in a third-party integrated ride-hailing platform (*31*). The study demonstrated that the proposed method can mitigate dispatching conflicts between platforms and enhance overall market efficiency, resulting in a higher order response rate, increased market revenue, and lower total travel distances.

However, these studies have predominantly focused on the supply (drivers) and demand (riders) dynamics, paying relatively less attention to the intricacies of cross-platform rider-rider matching. In contrast, our paper emphasizes the shareability of riders among platforms.

Our Contributions

To summarize, most studies have focused exclusively on a monopolistic matching environment, without examining how ride-sharing services may be improved by sharing riders between different platforms. Additionally, existing collaboration papers focus more on the supply management side rather than on rider shareability. To partially bridge these gaps, the contributions of this paper to the literature are as follows: 1) developed a graph-based framework with dynamic edge weights and maximum weighted matching method to match ride-share users; 2) proposed Shapley-value-based collaborating strategies for ride-sharing platforms in sharing users; and, 3) examined the impacts of collaboration over competition under varying levels of information transparency and varying levels of market segmentation.

METHODOLOGY

In this section, we first discuss the trip fare and profit allocation, then the geographical and temporal adjacency of riders, and the rider-rider graph (RR-G) concepts. We then present the market partition, which includes full competition, full collaboration, and rational collaboration. Finally, we present the method to find maximum weighted matching pairs in the constructed general graphs

under different market behaviors.

Trip Fare and Profit Allocation

Demand is spatially and temporally stochastic, with riders selecting platforms based on heterogeneous preferences and factors. A trip request from a given rider r_i is distinguished by the following four characteristics: $r_i = \{P_i, t_i, O_i, D_i\}$. Here, P_i is a categorical variable denoting the platform selected, t_i is the request time, O_i is the rider's origin, and D_i is the rider's destination. The platform then offers an upfront flat fare to this rider, f_i, based on the direct trip distance from his origin to destination, as defined in Equation (1). If a rider shares a trip with others, we assume for simplicity that the fare collected from each shared rider is the same as for single trips, although a discount could be given.

$$f_i = l_i(\alpha^d + \frac{\alpha^t}{\bar{v}}), \tag{1}$$

where l_i is the direct distance of r_i; α^d, α^t are the unit value of distance and unit value of time; and $\bar{v}$ is the average speed of the vehicles, which is assumed here to be a constant for simplicity.

Assuming the driver's cost is proportional to vehicle traveled distance and time, the profit each platform obtains from a single trip is defined in Equation (2), and the profit from a shared trip for rider pair (r_i, r_j) is defined in Equation (3).

$$p_i = f_i(1-o), \tag{2}$$

$$p_{ij} = f_i + f_j - l_{ij}(\alpha^d + \frac{\alpha^t}{\bar{v}})o, \tag{3}$$

where p_i is the profit out of r_i; o is the driver payout rate; l_{ij} is the travel distance of the shared trip; and f_j is the fare from r_j.

The profits from inter-platform shared trips are distributed to different platforms based on the Shapley value method (*32*), a game-theory-based profit allocation scheme defined in Equation (4). In our collaborative game, the shareable riders are considered the players, denoted as N. Each successfully served solo rider or shared rider pair, such as (r_i, r_j), is considered a coalition S. The profit gained for the platforms is the value of this coalition, denoted as $v(S)$.

$$\phi_i(v) = \sum_{S \subseteq N \setminus \{i\}} \frac{|S|!(|N|-|S|-1)!}{|N|!} \left[v(S \cup i) - v(S)\right], \tag{4}$$

where $\phi_i(v)$ is the profit allocated to player i; $v(S \cup i)$ is the value of the coalition with the addition of player i; summation over $S \subseteq N \setminus \{i\}$ considers all coalitions without player i.

When we restrict at most two riders in a shared trip, the matching decision becomes a two-player cooperative game, and the Shapley values ϕ_{r_i} and ϕ_{r_j} are simplified as:

$$\begin{aligned} \phi_{r_i} &= \frac{1}{2}\left(v(\{r_i\}) - v(\{\emptyset\})\right) + \frac{1}{2}\left(v(\{r_i, r_j\}) - v(\{r_j\})\right), \\ \phi_{r_j} &= \frac{1}{2}\left(v(\{r_j\}) - v(\{\emptyset\})\right) + \frac{1}{2}\left(v(\{r_i, r_j\}) - v(\{r_i\})\right), \end{aligned} \tag{5}$$

where $v(\{r_i\})$ is the value (profit) out of i^{th} solo trip; $v(\{\emptyset\})$ is the value (profit) of no trips, and is 0; $v(\{r_i, r_j\})$ is the value (profit) of the shared trips.

Feasible Pairs

Many trips are 'similar' regarding origins, destinations, and time, and therefore could be aggregated into fewer vehicles. Here, we define pairs of riders sharing their trips as feasible pairs, and two steps are needed to find them:

First, a sliding window technique (*20*) segments trip requests into small batches. As shown in Figure 1, the sliding window (sw^t) is an ε-length time window (e.g., $\varepsilon = 5$ minutes) that moves over time. The moving step, s, of this window can be any integer within $[1, \varepsilon]$. The riders with the request time inside t^{th} time window, $[t-\varepsilon, t]$, are considered active riders for pairing.

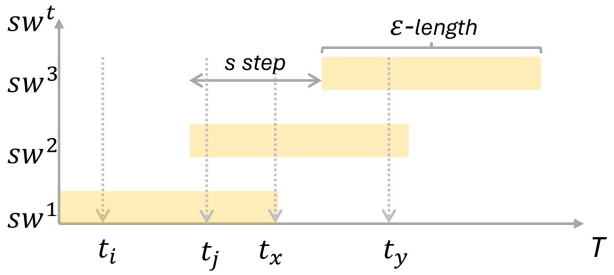

Note: t_i, t_j, t_x, t_y are rider arrival times, sw^t is the t^{th} sliding window, and ε, s are its length and moving step.

FIGURE 1: Illustration of a Sliding Window

Second, we determine if there exists a shortest path for two active riders. Since we assume at most two riders (e.g., r_i and r_j) can share their trips, only four possible pick-up and drop-off sequences exist: $O_i\underline{O_jD_j}D_i$, $O_j\underline{O_iD_i}D_j$, $O_iO_jD_iD_j$, and $O_jO_iD_jD_i$, as depicted in Figure 2. The underlined sequence is the trip segment same as direct single trips, where no detour distance is encountered. The shortest travel distance of the path, denoted as l_{ij}, is the smallest length of four possible paths. However, whether this ride-sharing pair is feasible is checked with the following three constraints:

- Constraint 1 (C_1): **Waiting time constraints.** To minimize the wait time for riders after booking, a waiting time threshold, τ, is set for each rider to be picked up.
$$l_{O_iO_j} \leq \bar{v}\tau. \tag{6}$$
where $l_{O_iO_j}$ is the travel distance between origins of r_i and r_j, assuming r_i is picked up first.
- Constraint 2 (C_2): **Detour distance constraints.** To prevent excessively long travel times, only a certain proportion of a passenger's direct trip distance is acceptable as an additional distance for a shared trip.
$$\frac{l_{O_xD_x} - l_x}{l_x} \leq \gamma, \ \forall x \in i, j, \tag{7}$$
where l_x and $l_{O_xD_x}$ are the direct trip distance and the distance between the origin and destination of rider x ($x \in \{i, j\}$) in a shared trip (which may include a partial detour), respectively; and γ is the fixed detour factor.
- Constraint 3 (C_3): **Profit constraints.** The profit from shared trips should be no less than the sum of profits from single trips.
$$p_i + p_j \leq p_{ij}. \tag{8}$$
where p_{ij} is from Equation (3), and p_i and p_j are from Equation (2).

Checking the constraints for every two active riders with Equations (6)–(8), the indicators (0 or 1) for feasible pairs are recorded in an indicators matrix, denoted as I^t, defined in Equation (9).

$$I^t = \left\{ I^t_{ij} \mid I^t_{ij} = \begin{cases} 1 & \text{if } C_1 \cap C_2 \cap C_3, \\ 0 & \text{otherwise} \end{cases} \text{ and } \forall i, j \text{ such that } r_i, r_j \in \text{sw}^t \right\}. \tag{9}$$

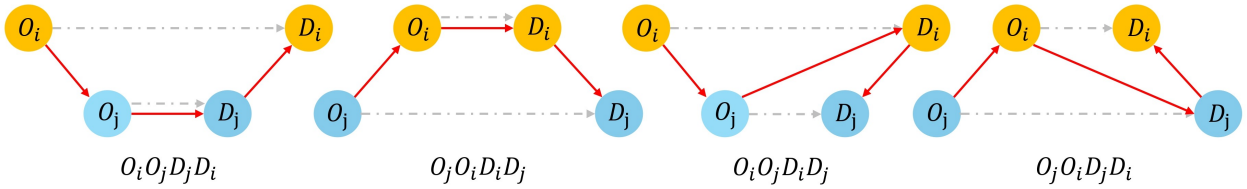

Note: The locations do not represent the actual locations but merely illustrate the path sequences. Dashed grey arrows show the direct single trip path, while the solid red arrows represent the shared trip path.

FIGURE 2: Illustration of Path Sequences

Rider-Rider Graph

A representative rider-rider graph (RR-G) is an undirected weighted graph that represents the adjacency relationships among riders over a specific period.

Vertices

V^t represents the active riders set in the t^{th} sliding window sw^t, and the number of vertices, $|V^t|$, is the number of active riders in that window. k different colors are assigned to the vertices, representing the riders belonging to k different platforms.

Edges

The edge set is a set of unordered pairs of vertices, denoted as $E^t \subseteq \{(x,y) \mid x,y \in V^t \text{ and } x \neq y\}$. Each edge is associated with two distinct vertices and is connected with a weight representing the adjacency relationships between riders. The weight of an edge in our graph is dynamic, as defined by Equation (10). It consists of two parts: the profit of the shared trip and the waiting time of the connected riders. The elements in the indicator matrix, I^t_{ij}, are used to decide whether an edge exists in the graph. With the sliding window, each additional waiting step increases a rider's connection weight, prioritizing longer waits and reducing overall waiting time.

$$w_{ij} = I^t_{ij}\left[p_{ij} + (t^w_i + t^w_j)\ \alpha^t\right], \tag{10}$$

where t^w_i and t^w_j are the waiting time of rider r_i and rider r_j, I^t_{ij} is from Equation (9).

Thus, the RR-G, $G^t = (V^t, E^t)$, can be constructed with the elements introduced above. Modifications on G^t are made in the next subsections to represent different market behaviors. A schematic RR-G is presented in Figure 3, where we considered two platforms in the system. On the left is the requested trip queue in the sliding window of $[0,5]$, and on the right is the constructed $G^{t=5}$.

The Ride-sharing Market

The status quo ride-share market is primarily dominated by only a few TNC platforms with differentiated services, presenting an oligopolistic market. For instance, the ride-sharing market in Manhattan is dominated by Uber and Lyft, creating a special scenario of oligopoly: a duopoly market. Under the current market structure, there is no collaboration among TNC platforms, only full competition behaviors. However, we propose methods to construct the RR-G and analyze the performance under competition and collaboration (both full and rational) behaviors.

Full Competition

With full competition behavior, the platforms operate independently. Suppose an RR-G of the whole ride-sharing system at the t^{th} sliding window is represented as $G^t = (V^t, E^t)$. Each platform owns only an induced sub-graph of this G^t, denoted as H^t_i. The induced sub-graph contains only a

RID	Platform	Time	OID	DID	Edge Weight
1	0	0	1	5	6.55
2	0	1	3	1	3.17
3	0	2	4	5	5.67
4	0	3	5	2	3.21
5	1	0	1	1	0.19
6	1	2	1	1	0.33
7	1	3	1	6	3.01
8	1	3	3	3	0.31
9	1	4	5	2	3.37
10	1	5	5	6	4.09

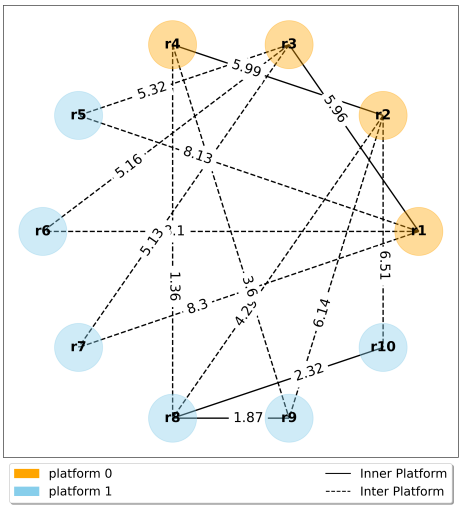

Note: Solid lines show feasible pairs within platforms, and dashed lines show those between platforms.

FIGURE 3: Rider Requests and Schematic Rider-Rider Graph at a Single Time-Step

subset of vertices from G^t and all the edges from G^t that connect vertices only within this subset. If there are k different platforms, there will be k induced sub-graphs, and each is defined in Equation (11). The weight of edges is calculated using Equation (10), except for all r_i and r_j belonging to different platforms, which are modified to 0.

$$H_i^t = (V_{H_i}^t, E_{H_i}^t), \text{ where } V_{H_i}^t = \{x \mid x \in P_i\} \text{ and } E_{H_i}^t = \{(x,y) \mid x,y \in P_i\}, \tag{11}$$

where P_i represents the i^{th} platform ($i \in [1,k]$), $V_{H_i}^t$ is the vertex set with riders belonging to the i^{th} platform ($V_{H_i}^t \subseteq V^t$), and $E_{H_i}^t$ is the edge set connecting only riders within the platform ($E_{H_i}^t \subseteq E^t$). Vertices x, y are riders in P_i.

Full Collaboration

Full collaboration assumes all providers share all resources as if they were one provider to optimize the entire system's operation. Under this behavior, the collaborative graph $C^t = (V_C^t, E_C^t)$ includes all vertices and edges from the RR-G, with weights defined by Equation (10):

$$C^t = (V_C^t, E_C^t), \text{ where } V_C^t = V^t \text{ and } E_C^t = E^t. \tag{12}$$

where V_C^t is the vertex set with active riders in the current sliding window, and E_C^t is the edge set with edges connecting both inter-platform riders and intra-platform riders.

Rational Collaboration

Rational collaboration, on the other hand, differs from the full collaboration scenario in that two additional conditions need to be met before a rider may be shared with another platform: 1) each provider has some control over rider information transparency, which controls the extent to which the rider's information is exposed across the market while collaborating; and, 2) each platform checks the up-front profit—calculated using the Shapley value—of sharing a rider with another platform before allowing it to be shared, with Equation (4)–(5). Trips may only be shared if they fit within the information transparency provision and are financially feasible to do so. The indicator matrix for the qualified edges connecting r_i and r_j in this rational collaboration scenario, derived from Equation (10), is updated as follows:

$$I_{ij}^t = \mathbb{1}_{ij}\left((\phi_{r_i}^{\text{inter}} \geq \phi_{r_i}^{\text{inner}}) \wedge (\phi_{r_i}^{\text{inter}} \geq p_i) \wedge (\phi_{r_j}^{\text{inter}} \geq p_j) \wedge (\phi_{r_j}^{\text{inter}} \geq \phi_{r_j}^{\text{inner}})\right) I_{ij}^t \quad (13)$$

where $\mathbb{1}_{ij}$ is the indicator function. $\phi_{\cdot}^{inter}$ and $\phi_{\cdot}^{inner}$ are the inter-platform upfront profit and inner-platform profit for r_i or r_j in the pair (i, j), calculated using the Shapley value method.

Then the weight of edges is calculated with the updated indicator matrix and Equation (10). And the rational collaborative RR-G, denoted as $RC^t = (V_{RC}^t, E_{RC}^t)$, is defined as:

$$RC^t = (V_{RC}^t, E_{RC}^t), \text{ where } V_{RC}^t = \{x \mid x \in P_i \wedge P_j\} \text{ and } E_{RC}^t = \{(x,y) \mid x,y \in P_i \wedge P_j\}, \quad (14)$$

where V_{RC}^t is the vertex set, containing all active riders in all platforms ($V_{RC}^t = V^t$); and E_{RC}^t is the edge set that contains all inner-platform edges and partial inter-platform edges ($E_{RC}^t \subseteq E^t$).

Maximum Weighted Matching (MWM)

The optimum ride-sharing solutions are also provided dynamically within each sliding window. Using RR-Gs under different market behaviors— $H^t = (V_H^t, E_H^t)$, $C^t = (V_C^t, E_C^t)$, and $RC^t = (V_{RC}^t, E_{RC}^t)$ —three matching sets M_H, M_C, and M_{RC} are decided by:

$$\begin{aligned} \max \quad & W(G) = \sum_{E_{ij} \in M} w(E_{ij}) \\ \text{s.t.} \quad & E_{ij} \cap E_{xy} = \emptyset, \quad \forall E_{ij}, E_{xy} \in M, \\ & M \subseteq E, \\ & w(E_{ij}) = w_{ij}, \end{aligned} \quad (15)$$

where G is one of the defined RRGs, $W(G)$ is the maximum weight of graph, and E is the corresponding edge set of the RR-G. M is the matching set to be assigned, which is the subset of E.

Finding the augmenting path is the core of finding the maximum weighted matching in a general graph, which is defined as an alternating path that starts and ends with unmatched vertices and alternates between edges not in M and edges in M. We utilized the technique of finding a maximum weighted matching in general graphs developed by Galil (*27*), which employs a primal-dual method. Finding the matching (edge set) is a primal solution, and the dual solution is an assignment of dual variables u_i, u_j corresponding to vertices. With the solution of rider pairs, and given the large number of available drivers in TNCs, dispatching the nearest driver to the itinerary instantly is feasible. Therefore, in the following, we assume all paired-up riders or solo riders can be matched with available drivers.

EMPIRICAL EXPERIMENT

The experiment is designed to examine the feasibility of the proposed model and analyze the impact of different market behaviors on the ride-sharing system's performance under varying market shares and information transparencies. This section details the data, experimental designs, parameters, and simulation steps.

Data

TLC trip data (*33*) from Manhattan, NYC are used as system inputs. From 2019 to 2023, the proportion of shared trip requests dropped significantly from 16% to 2%, according to the data in Table 1. Due to this shift, the most recent data from February 2023 were considered here. Figure 4 shows the daily and five-minute aggregated counts of requested single and shared trips. Most days see around 180,000 single trip requests and 3,250 shared trip requests, with about 750 single trip requests and 10 shared trip requests every five minutes. This data indicates that current shared

ride services have very few candidates. To maximize potential benefits from the current market, we focus on February 4th, 2023, the day with the highest number of shared trip requests, totaling 4,235.

The TLC trips are encoded with locations in taxi zones (*33*). To simulate travel distances more precisely, we used the GeoPandas (*34*) and OSMNX (*35*) Python packages to decode the origins and destinations from 63 zones in Manhattan to 4,589 intersections in the roadway network. The all-to-all distance matrix was queried and recorded.

TABLE 1: Summary of Manhattan TNC Trips in February 2019 VS February 2023

TNC (Year)	Realized Trips	Shared (%)	Base Fare ($)	Unit Fare ($/mile)	Unit Fare ($/min)	Avg. Wait Time (min)	Avg. Trip Distance (mile)	Avg. Direct Time (min)
UberX (2019)	3,526,943	–	2.40	1.42	0.54	4.29	2.52	14.92
UberPool (2019)	837,247	80.11	1.42	1.06	0.06	6.88	3.01	17.88
UberX (2023)	4,196,579	–	4.09	1.76	0.64	4.05	2.56	14.71
UberPool (2023)	55,491	45.18	3.43	0.81	0.50	6.45	4.47	22.13
Lyft (2019)	991,262	–	2.99	1.61	0.45	3.89	2.65	14.74
LyftLine (2019)	676,557	79.36	2.48	1.27	0.09	5.96	3.18	18.89
Lyft (2023)	1,136,579	–	3.96	1.62	0.58	4.64	2.70	14.87
LyftLine (2023)	45,770	34.64	3.96	0.65	0.52	12.48	4.71	22.89

Note: UberX, Lyft: single trip service; UberPool, LyftLine: shared trip service
all fare-related parameters were estimated with linear regression and statistically significant p-values.

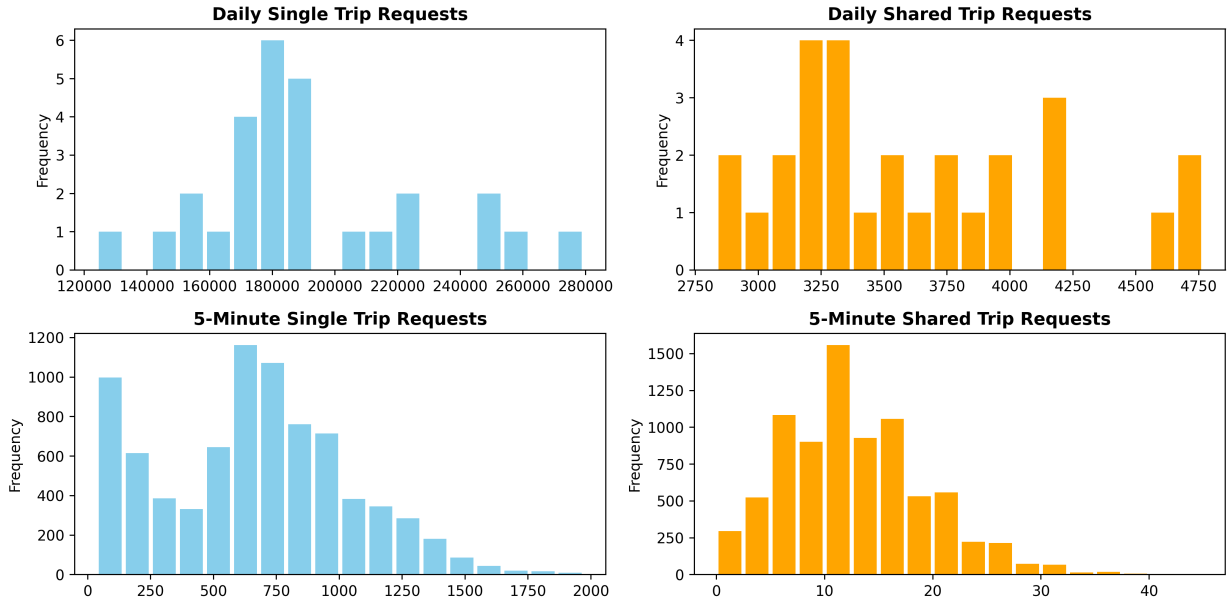

FIGURE 4: Distribution of Aggregated (Every 5-minutes) Trips in February, 2023

Design

In the experiment, two varying parameters are market share and rider information transparency. Three types of market shares are examined under low (30%), equal (50%), and high (70%) conditions for one platform (referred to as platform 0) in a market comprising two platforms (0 and 1).

The rider information transparency indicates the different levels of control over the rider's information sharing with other platforms in rational collaborations, also viewed as an indicator of the platform's willingness to collaborate. Five different levels of rider information transparency are explored for platform 0: $[0.2, 0.4, 0.6, 0.8, 1.0]$.

Ten replications of the simulation are conducted to ensure the robustness and reliability of the results. Parameters used in the simulation are listed and explained in Table 2. Control parameters are fixed constant for all designs, including ε, s, τ, o, γ, $\bar{v}$, α^d, and α^t. Notice that these parameters could vary across different service quality objectives. However, this is not the key focus of this paper, so we hold them constant.

Detailed steps of a single replication are as follows: the time horizon of a single replication is set to $H = 1440$ minutes (24 hours), and the sliding window moves over a day. We set both the length and the moving step of the sliding window to 5 minutes, also defined as non-overlapping windows. In the beginning, $t = 0$, the daily trip requests, Q^0, are loaded into the simulator, encompassing initial features such as the arrival time, the platform they requested from, origins, and destination. The trip fares are calculated using Equation (1), with $\alpha^d = 1$ and $\alpha^t = 0.2$. At this stage, some randomness could be introduced into the rider's selection of platforms, based on a defined market share of platforms, P. Although all data are loaded into the simulator at the same time, trips are marked as active to serve only when they fall within the sliding window, sw^t. At each time step, the following steps are conducted:

1. Update the queue, Q^t, including the status of riders (inactive, active, served), waiting time of unserved riders, etc.
2. Gather all un-served requests from active riders to calculate the shareability indicator matrix I, with Equations (6)–(9).
3. Construct vertices and weighted edges in three distinct RR-Gs: the competitive graph H^t, the full collaborative graph C^t, and the rational collaborative graph RC^t using Equations (10)–(14).
4. Compute and allocate upfront profits from feasible pairs to the corresponding platforms based on the Shapley value method, in Equations (4)–(5).
5. Check, determine, and record the maximum weighted matching set within the constructed graphs based on Equation (15).
6. Update the queue Q^t with the matching records and record the profits from both inter-platform and intra-platform matches to corresponding platforms.

Evaluation Metrics

Six performance metrics were used to quantify the performance:

- **Share rate:** percentage of rider requests served as shared riders.
- **Platform profit:** total revenue generated by the trip fare minus the operational costs.
- **Vehicle travel distance:** distance traveled by vehicles in serving riders.
- **Shared trip distance:** trip distance when both shared riders are on board.
- **Passenger detour distance:** additional distance a passenger has to travel due to sharing a ride with others, compared to a direct trip.
- **Passenger waiting time:** time a rider waits from requesting a ride until being offered a trip.

TABLE 2: Summary of parameters in ride-sharing simulation

Notation	Interpretation	Value
n	Number of replications	10
H	Horizon (minute)	1440
t	Time step	$[0,H]$
M	The number of Platforms	2
Q^t	Riders' trip request queue at certain time	$[r_1,r_2,...,r_i]$, $i \in [1,4235]$
ε	Length of sliding window (minute)	5
s	Moving step of sliding window (minute)	5
sw^t	Sliding window (minute)	$[t-\varepsilon,t]$
P	Market Share	[0.3, 0.7], [0.5, 0.5], [0.7, 0.3]
Θ	Rider information transparency	[0.2, 0.4, 0.6, 0.8, 1.0]
τ	Maximum waiting time (minute)	10
o	Driver payout factor	0.5
γ	Maximum detour factor	0.4
$\bar{v}$	Velocity (mph)	30
α^d	Value of distance (vod) ($/mile)	1
α^t	Value of time (vot) ($/minute)	0.2

RESULTS

This section presents the results of experiments conducted under various designs and analyzes the outcomes across all three market behaviors.

Share Rate

Two share rate results are explored: one over a 5-minute horizon and another over a one-day horizon. To eliminate the influence of unrelated parameters, we control the market share across the two platforms to match a real-world scenario (58% and 42%) and set the rider information transparency of both platforms to 100%. This setting for the control variables remains consistent until the sensitivity analysis subsection.

Figure 5 shows the MWM results of riders within a specific 5-minute time horizon. Each node (from r_0 to r_{22}) represents a rider. Solid black lines indicate potential intra-platform matches, while dashed black lines indicate potential inter-platform matches. Since rational collaboration has more constraints on collaboration than full collaboration, there are fewer dashed lines. Under the full competition scenario, in Figure 5(a), only solid lines can be selected for the matching set. Under both collaboration scenarios, in Figure 5(b) and Figure 5(c), both solid and dashed lines can be selected. Red lines indicate optimum matches. In the competitive market, in Figure 5(a), the optimum matching pairs are $M_1 = \{r_0r_{15}, r_3r_{20}, r_5r_9, r_{21}r_{22}\}$ with a match rate of 36%; in the full collaboration, in Figure 5(b), the optimum matching is $M_2 = \{r_0r_{15}, r_2r_4, r_5r_{10}, r_6r_3, r_9r_{17}, r_{13}r_{20}, r_{21}r_{22}\}$ with a match rate of 64%. In the rational collaboration, in Figure 5(c), the optimum matching is $M_3 = \{r_0r_{15}, r_2r_4, r_5r_{10}, r_6r_3, r_9r_{17}, r_{21}r_{22}\}$ with a match rate of 54%. This result provides an overview of how matching differs under different scenarios. The average benefits are quantified over a one-day horizon and presented in the next figure.

Figure 6 illustrates the riders' share rate over one day, segmented into four time intervals: 0-5 hours, 6-11 hours, 12-17 hours, and 18-23 hours. The grey bars show the total number of

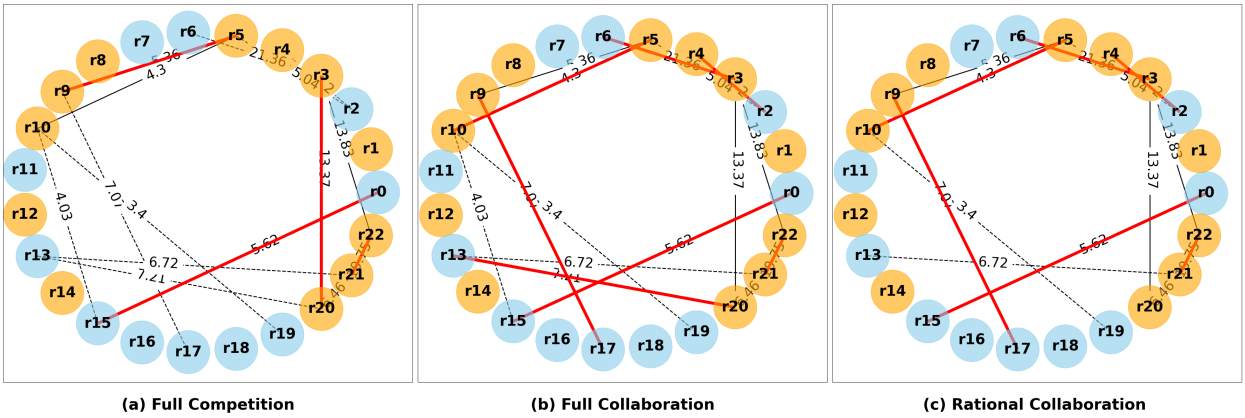

FIGURE 5: Maximum Weighted Matching Result for Riders within one sliding window in (a) Competitive Market, (b) Fully Collaborative Market, and (c) Rational Collaborative Market

shared trip requests, and the colored bars present the number of realized shared trips under the three scenarios mentioned above. Additionally, the corresponding share rates in each scenario are depicted as dashed lines. The benefits of collaboration are evident: the share rate increases by approximately 15% under full collaboration. Additionally, full collaboration results in a marginally higher share rate (2%) than the rational collaboration scenario. This is because the full collaboration scenario maximizes shared trips without being constrained by individual platform profits. In contrast, rational collaboration only facilitates inter-platform matching if the profit exceeds that of intra-platform matching or a single rider traveling alone on their platform. The results demonstrate that collaboration enhances share rates, and rational collaboration can achieve performance levels close to those of full collaboration under our settings, where all platforms operate as a single entity.

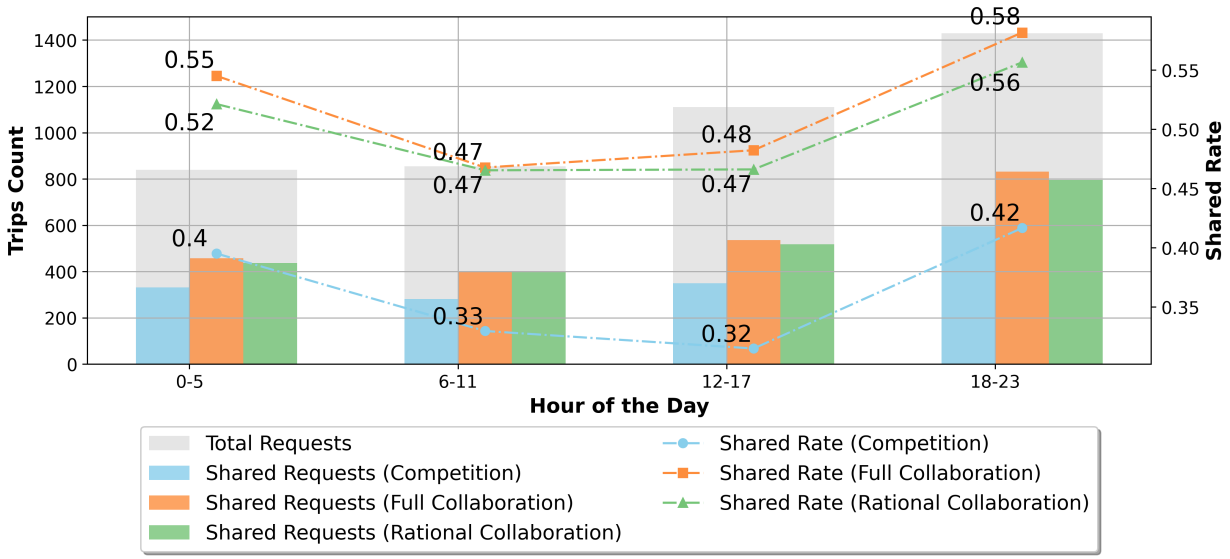

FIGURE 6: Shared Rate over One Day

Platform Profit

Figure 7 presents the profit benefits of the ride-sharing system. The competition with the shared trips scenario (Figure 7 (b)) shows higher profit than single trips (Figure 7 (a)), suggesting that promoting shared trips is more profitable under our matching constraints. Both platforms experience profit growth when the market transitions from competitive behavior to a fully collaborative one. The full competition scenario (Figure 7 (c)) reveals the highest profits, demonstrating that full resource sharing and coordination maximize system efficiency and profitability. The rational collaboration scenario (Figure 7 (d)) also yields substantial profits, albeit slightly lower than full collaboration, validating the feasibility of our proposed collaboration way. Besides, platform 0 consistently achieves higher profits than platform 1, reflecting its larger market share.

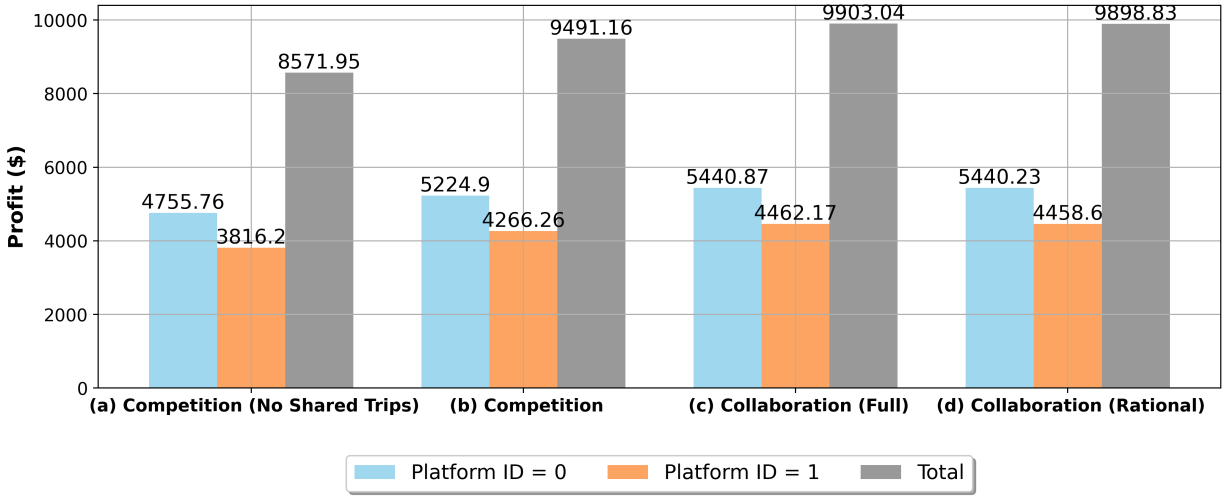

FIGURE 7: System Profit under Different Modes

Trip Characteristics

TABLE 3: Comparison of Service Quality Across Different Scenarios

Scenario	Vehicle Distance	Shared Distance	Detour Distance	Wait Time
Competition	5.65	2.59	0.454	3.84
Rational Collaboration	5.48	2.65	0.443	3.71
Full Collaboration	5.52	2.61	0.451	3.69

Table 3 presents several metrics for shared trips from the same experiment mentioned above to evaluate service quality performance across the three market behaviors. Variations of these four metrics under different experiment designs can also be seen in Figure 8. Vehicle distance represents the distance from the first passenger pickup to the last passenger drop-off, while shared distance is when both passengers are on board. A lower shared distance typically results in a higher vehicle distance and detour distance for successfully shared trips. For example, rational collaboration has a shared distance of 2.65 miles compared to 2.61 miles in full collaboration, a lower average vehicle

travel distance of 5.48 miles versus 5.52 miles, and a lower detour distance of 0.443 miles versus 0.451 miles. But the differences are small, which are less than 0.1 mile. Generally, the performance of full and rational collaboration is very similar and is better than competitive behavior.

Sensitivity Analysis

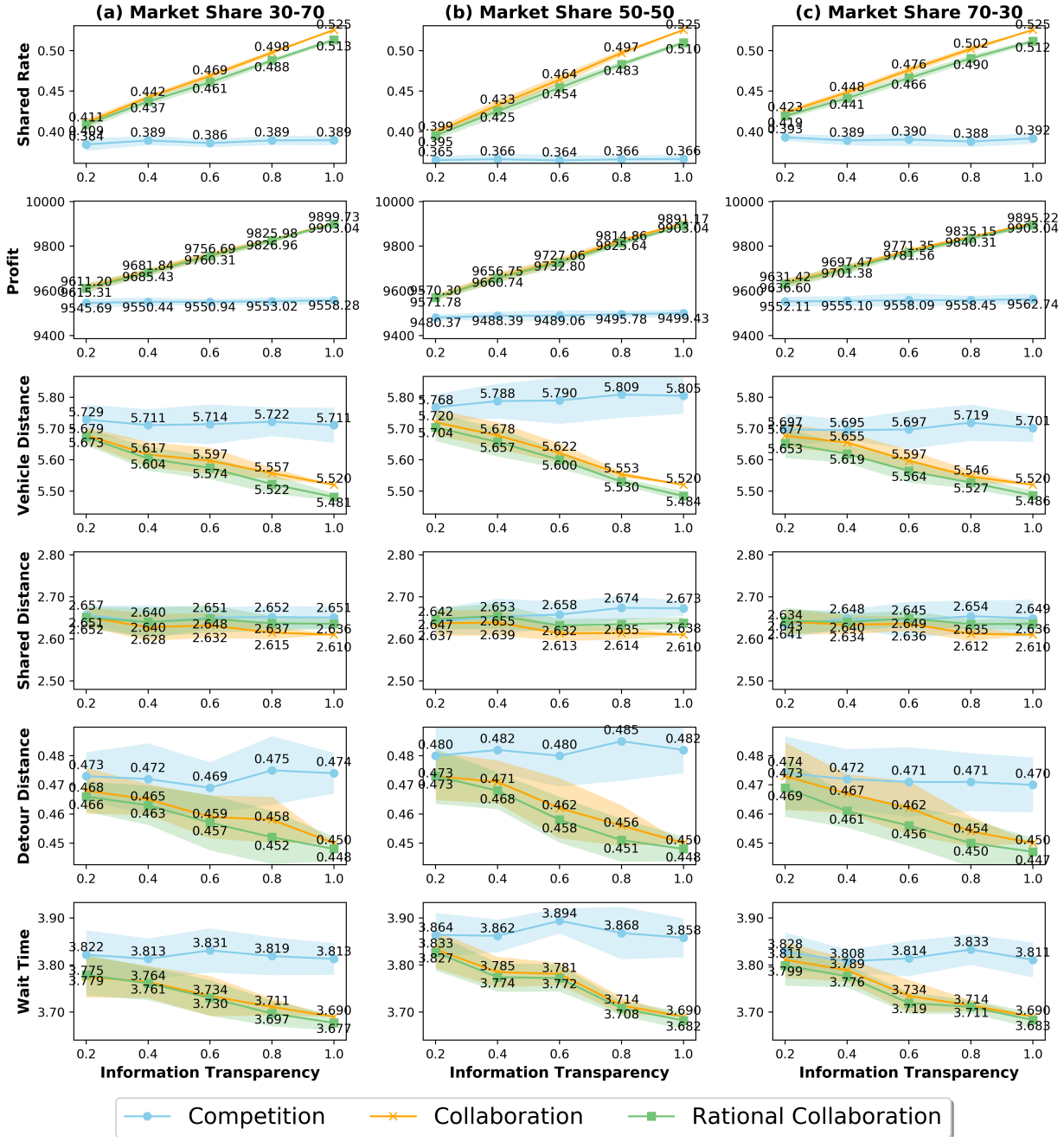

FIGURE 8: Influence of Market Share and Information Transparency

A sensitivity analysis on the influence of market share and rider information transparency is analyzed, which was held fixed in the previous results. The system performance of three market behaviors under different levels of market share and rider information transparency are explored.

Figure 8 shows the whole system's performance under different experiment designs. The six rows show the results of the six metrics we used to evaluate the system. The three columns represent varying levels of market shares, where riders select platforms at ratios of [30%, 70%], [50%, 50%], and [70%, 30%] for platform 0 and platform 1, respectively. In each sub-plot, different levels of Θ are controlled over platform 0, while the value for the other platform is set to 1. The blue, orange, and green lines show the average performance over ten replications of competition, collaboration, and rational collaboration, respectively. The shaded areas represent the standard deviations across the replications.

First, the effects of rider information transparency (Θ) are discussed. Overall, the general trend across all subplots is that increasing Θ raises the share rate and system profit, while it reduces average vehicle travel distances, detour distances, and passenger waiting times across all market behaviors. This indicates that higher rider information transparency generally leads to better system performance. The shared trip distances, however, do not show obvious changes, as the shaded areas representing standard deviations of different behaviors overlap significantly. Under a low transparency level, the improvement in the system's performance under collaboration behaviors is limited compared to a fully competitive market. However, when the transparency level is high, the improvement is notable. For instance, in the first row of Figure 8(b), when the market share is equal and $\Theta = 0.2$, the improvement in the system's share rate is only around 3% for both rational and full collaboration compared to the competition results. However, when $\Theta = 1$, the improvement is notable, around 15% for rational collaboration and 16% for full collaboration. Therefore, a higher information level generally leads to better system performance.

Second, the effects of market share levels are discussed. Generally, when the platform with a high market share provides high rider information transparency, it helps achieve better system performance than a platform with a lower market share. For instance, in the first row of Figure 8(c), when $\Theta = 0.8$, the system's shared rate is 50.2%, compared with 49.8% and 49.7% for the corresponding situation in Figure 8(a) and Figure 8(b). When the market share is equal, the influence of rider information transparency is the most significant. As Θ increases from 0.2 to 1, the equal market share scenario shows the largest changes in all metrics (expect shared distance) compared to the other two market share conditions. For instance, under the rational collaboration scenario with $\Theta = 0.2$, the shared rates across all three market shares are 40.9%, 39.5%, and 41.9%, respectively. But towards the end when $\Theta = 1.0$, shared rates across all three market shares are the same, indicating the equal market has the largest improvement in share rates. This is because the requests are equally segmented into two matching pools, a larger information of transparency would help platforms collaborate and communicate.

Computation Time

Figure 9 presents the relationships between each of the number of edges, the graph creation time, and the graph matching time with the number of nodes in the created graph. The blue dots represent the full collaboration mode, while the orange dots present the rational collaboration mode. Figure 9(a) indicates that the number of edges in the rational collaboration mode is less than in the full collaboration mode. As seen, the greater the number of nodes, the sparser the graph becomes (the number of edges is less than half of the potential edges), which is advantageous for applying

graph-based methods to find the maximum matching. Figure 9(b) and Figure 9(c) show the time consumed for constructing graphs and finding the maximum matching of general graphs. Times are recorded each time the RR-G is operated in the sliding windows, averaged over a whole day. Each task theoretically has time complexities of $O(n^2)$ and $O(mn\log n)$, where m and n represent the number of edges and nodes, respectively. The experiment results demonstrate that the proposed graph-based collaboration method achieves results within an acceptable time.

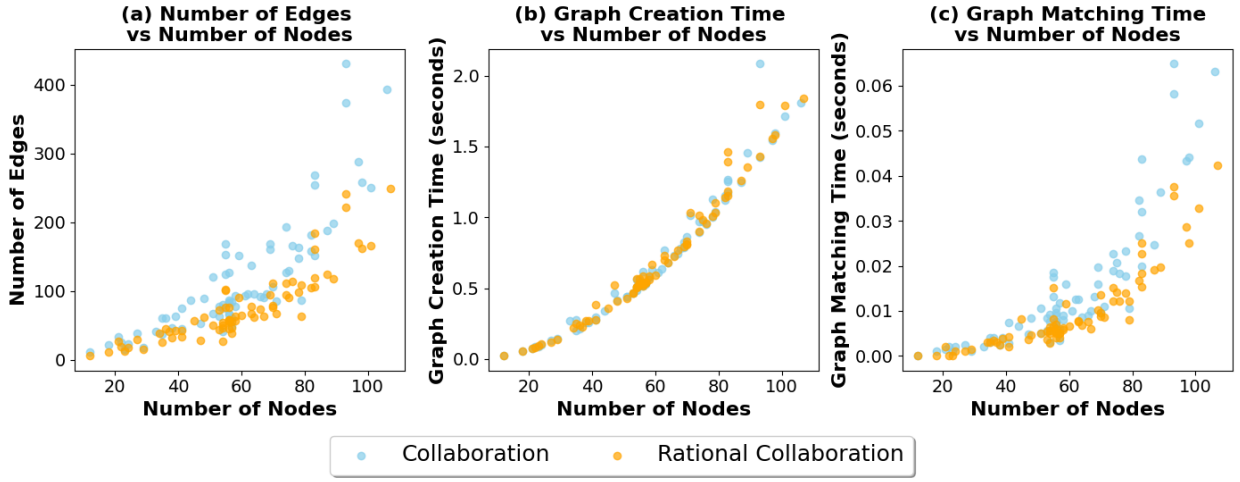

FIGURE 9: Computational Time with Scales of Nodes in Graph

CONCLUSION

This paper proposes a dynamic graph-based matching framework to identify potential shared trips across different platforms in a ride-sharing system. A comparative analysis of performances under collaborative versus competitive platform behaviors is conducted. The collaborative market is modeled in two ways: full collaboration, where the system operates as a unified entity; and rational collaboration, where platforms determine the profitability of the profit allocation and rider information transparency. An upfront profit allocation is calculated with the Shapley value method and used to compare inter-platform profit with other options, such as solo travel or sharing a trip with passengers from the same platform. This ensures both platforms' willingness to collaborate while maintaining individual platform profits. When constructing the graphs, requests are partitioned into sub-graphs (representing different platforms) and the adjacency of riders is constructed as edges. Different market behaviors are represented by different levels of constraint on inter-platform edges (between inter-platform riders). A fully competitive market prohibits inter-platform edges, while full collaboration allows all qualified inter-platform edges. Rational collaboration adopts an intermediate level of constraint. The Shapley value-based profit allocation method guides individual platforms in determining the existence of these inter-platform edges. Then with the constructed graphs, the maximum weighted matching method is utilized to find optimum matching. Six key metrics are analyzed: share rate, platform profit, and four service quality metrics. Additionally, sensitivity analysis on market share and rider information transparency is explored.

Our findings reveal that both full and rational collaboration improve share rates and total profit, reduce total vehicle travel distance, and enhance service quality (e.g., lower detour dis-

tance and shorter waiting times) compared to a fully competitive market. The collaborative market demonstrates economies of scale, as inter-platform feasible pairs increase the overall matching probabilities. Furthermore, rational collaboration boosts each platform's profit proportionate to its market share. The sensitivity analysis indicates that increasing rider information transparency generally enhances system performance by raising share rates and system profits while reducing average vehicle travel distances, detour distances, and passenger waiting times across all market behaviors. High transparency levels in collaborative markets significantly improve system performance compared to competitive scenarios. Besides, when a platform with a high market share provides high rider information transparency, it enhances overall system performance more effectively than a platform with a lower market share. Equal market share conditions benefit the most from greater transparency in a collaborative market.

Our work offers transportation practitioners an overview of the quantifiable benefits of shifting from a fully competitive market to a rational collaborative market, and ideally to a fully collaborative market. Although the matching parameters, such as maximum wait time, maximum detour constraints, and fare calculations, may differ from industry standards, they are consistently applied as control variables across all scenarios, ensuring reliable comparison results across different market behaviors. This shift could lead to a more sustainable and customer-friendly market environment, potentially setting new standards for service quality and economic viability in the ride-sharing industry. Future work may quantify the scale of benefits when the willingness to pool increases with the entire ride-hailing dataset. Besides, a trip-based graph partition method could be incorporated to accommodate larger graphs and enable parallel matching. Additionally, considering vehicle routing details could help optimize fleet size under a rational collaborative market.

ACKNOWLEDGEMENTS

This research was supported by NSF Grants CMMI-2052337.

AUTHOR CONTRIBUTIONS

The authors confirm their contribution to the paper as follows: study conception and design: X. Dong, J. Ventura, V. Gayah; simulation: X. Dong; analysis and interpretation of results: X. Dong, J. Ventura, V. Gayah; draft manuscript preparation: X. Dong, V. Gayah; All authors reviewed the results and approved the final version of the manuscript.

REFERENCES

1. Shaheen, S. and A. Cohen, Shared ride services in North America: definitions, impacts, and the future of pooling. *Transport reviews*, Vol. 39, No. 4, 2019, pp. 427–442.
2. Ferguson, E., The rise and fall of the American carpool: 1970–1990. *Transportation*, Vol. 24, No. 4, 1997, pp. 349–376.
3. Tafreshian, A., N. Masoud, and Y. Yin, Frontiers in service science: Ride matching for peer-to-peer ride sharing: A review and future directions. *Service Science*, Vol. 12, No. 2-3, 2020, pp. 44–60.
4. Qin, Z. T., H. Zhu, and J. Ye, Reinforcement learning for ridesharing: An extended survey. *Transportation Research Part C: Emerging Technologies*, Vol. 144, 2022, p. 103852.
5. Chan, N. D. and S. A. Shaheen, Ridesharing in North America: Past, present, and future. *Transport reviews*, Vol. 32, No. 1, 2012, pp. 93–112.
6. Heineke, K., B. Kloss, T. Möller, and C. Wiemuth, Shared mobility: Where it stands and where it's going. *McKinsey Center for Future Mobility*, 2021.
7. Salcedo, B., Pricing algorithms and tacit collusion, 2015.
8. Stigler, G. J., The economies of scale. *The Journal of Law and Economics*, Vol. 1, 1958, pp. 54–71.
9. Lehe, L., V. V. Gayah, and A. Pandey, Increasing returns to scale in carpool matching: Evidence from Scoop. *Transport findings*, 2021.
10. Liu, H., S. Devunuri, L. Lehe, and V. V. Gayah, Scale effects in ridesplitting: A case study of the City of Chicago. *Transportation Research Part A: Policy and Practice*, Vol. 173, 2023, p. 103690.
11. Liu, H., S. Devunuri, X. Dong, L. Lehe, and V. V. Gayah, Impact of competition on the scale effects in ridesplitting: A case study of Manhattan. In *103rd Annual Meeting of the transportation Research baord*, National Academies of Engineering, 2024.
12. Hu, W., K. Browning, and K. Zraick, Uber partners with yellow taxi companies in N.Y.C. *The New York Times*, 2022.
13. Daus, M. W., *The Uber-Taxi partnership: regulatory evolution spaws a new transportation species!* https://www.blackcarnews.com/article/the-uber-taxi-partnership-regulatory-evolution-spawns-a-new-transportation-species, 2022.
14. Ke, J., H. Yang, H. Wang, and Y. Yin, *Supply and demand management in ride-sourcing markets*. Elsevier, 2023.
15. Daganzo, C. F., Y. Ouyang, and H. Yang, Analysis of ride-sharing with service time and detour guarantees. *Transportation Research Part B: Methodological*, Vol. 140, 2020, pp. 130–150.
16. Ouyang, Y., H. Yang, and C. F. Daganzo, Performance of reservation-based carpooling services under detour and waiting time restrictions. *Transportation Research Part B: Methodological*, Vol. 150, 2021, pp. 370–385.
17. Dong, X., H. Liu, and V. V. Gayah, An analytical model of many-to-one carpool system performance under cost-based detour limits. *International Journal of Transportation Science and Technology*, 2024.
18. Masoud, N. and R. Jayakrishnan, A decomposition algorithm to solve the multi-hop peer-to-peer ride-matching problem. *Transportation Research Part B: Methodological*, Vol. 99, 2017, pp. 1–29.

19. Alisoltani, N., L. Leclercq, and M. Zargayouna, Can dynamic ride-sharing reduce traffic congestion? *Transportation research part B: methodological*, Vol. 145, 2021, pp. 212–246.
20. Datar, M., A. Gionis, P. Indyk, and R. Motwani, Maintaining stream statistics over sliding windows. *SIAM journal on computing*, Vol. 31, No. 6, 2002, pp. 1794–1813.
21. Simonetto, A., J. Monteil, and C. Gambella, Real-time city-scale ridesharing via linear assignment problems. *Transportation Research Part C: Emerging Technologies*, Vol. 101, 2019, pp. 208–232.
22. Alonso-Mora, J., S. Samaranayake, A. Wallar, E. Frazzoli, and D. Rus, On-demand high-capacity ride-sharing via dynamic trip-vehicle assignment. *Proceedings of the National Academy of Sciences*, Vol. 114, No. 3, 2017, pp. 462–467.
23. Agatz, N., A. Erera, M. Savelsbergh, and X. Wang, Optimization for dynamic ride-sharing: A review. *European Journal of Operational Research*, Vol. 223, No. 2, 2012, pp. 295–303.
24. Duan, R. and S. Pettie, Linear-time approximation for maximum weight matching. *Journal of the ACM (JACM)*, Vol. 61, No. 1, 2014, pp. 1–23.
25. Agatz, N. A., A. L. Erera, M. W. Savelsbergh, and X. Wang, Dynamic ride-sharing: A simulation study in metro Atlanta. *Transportation Research Part B*, Vol. 9, No. 45, 2011, pp. 1450–1464.
26. Santi, P., G. Resta, M. Szell, S. Sobolevsky, S. H. Strogatz, and C. Ratti, Quantifying the benefits of vehicle pooling with shareability networks. *Proceedings of the National Academy of Sciences*, Vol. 111, No. 37, 2014, pp. 13290–13294.
27. Galil, Z., Efficient algorithms for finding maximum matching in graphs. *ACM Computing Surveys (CSUR)*, Vol. 18, No. 1, 1986, pp. 23–38.
28. Séjourné, T., S. Samaranayake, and S. Banerjee, The price of fragmentation in mobility-on-demand services. *Proceedings of the ACM on Measurement and Analysis of Computing Systems*, Vol. 2, No. 2, 2018, pp. 1–26.
29. Zhou, Y., H. Yang, J. Ke, H. Wang, and X. Li, Competition and third-party platform-integration in ride-sourcing markets. *Transportation Research Part B: Methodological*, Vol. 159, 2022, pp. 76–103.
30. Guo, X., A. Qu, H. Zhang, P. Noursalehi, and J. Zhao, Dissolving the segmentation of a shared mobility market: A framework and four market structure designs. *Transportation Research Part C: Emerging Technologies*, Vol. 157, 2023, p. 104397.
31. Wang, Y., J. Wu, H. Sun, Y. Lv, and J. Zhang, Promoting Collaborative Dispatching in the Ride-Sourcing Market With a Third-Party Integrator. *IEEE Transactions on Intelligent Transportation Systems*, 2024.
32. Shapley, L. S. et al., A value for n-person games, 1953.
33. NYC Taxi and Limousine Commission, *NYC TLC Trip Record Data*. https://www.nyc.gov/site/tlc/about/tlc-trip-record-data.page, 2024.
34. Jordahl, K., GeoPandas: Python tools for geographic data. *URL: https://github.com/geopandas/geopandas*, 2014.
35. Boeing, G., OSMnx: New methods for acquiring, constructing, analyzing, and visualizing complex street networks. *Computers, environment and urban systems*, Vol. 65, 2017, pp. 126–139.